

# Chapter 7

---

## Experimental demonstration of coarse-fine grooming in coarse-WDM architectures

This chapter concludes the practical investigations presented in this thesis by experimentally demonstrating the application of coarse-fine grooming across the access network described in chapters 4 and 5 by means of a readily-available wide-passband AWG router and RSOA-based ONUs terminated to a densely-penetrated PON. In particular, the polarisation dependency of the AWG and asymmetrical bidirectional behaviour observed through simulations, in addition with the OLT capability to provide CWs alongside burst-data with sufficient power to overcome total network losses while avoiding the saturation of the RSOAs have been experimentally evaluated to account for the wavelength dependency of the RSOA reflected power upstream. The inclusion of these parameters in defining the network power budget has provided an accountable conclusion on Rayleigh backscattering, in comparison with related architectural approaches.

### 7.1 Network architecture and experimental setup

A detailed diagram of the network architecture [1], incorporating the developed experimental setup is shown in Figure 7-1 (see appendix C.1 for a snapshot). It has been previously established that PDW shift could potentially impose a restriction in multi-wavelength operation over wide-passband AWG channels and therefore limit the routing performance of the entire

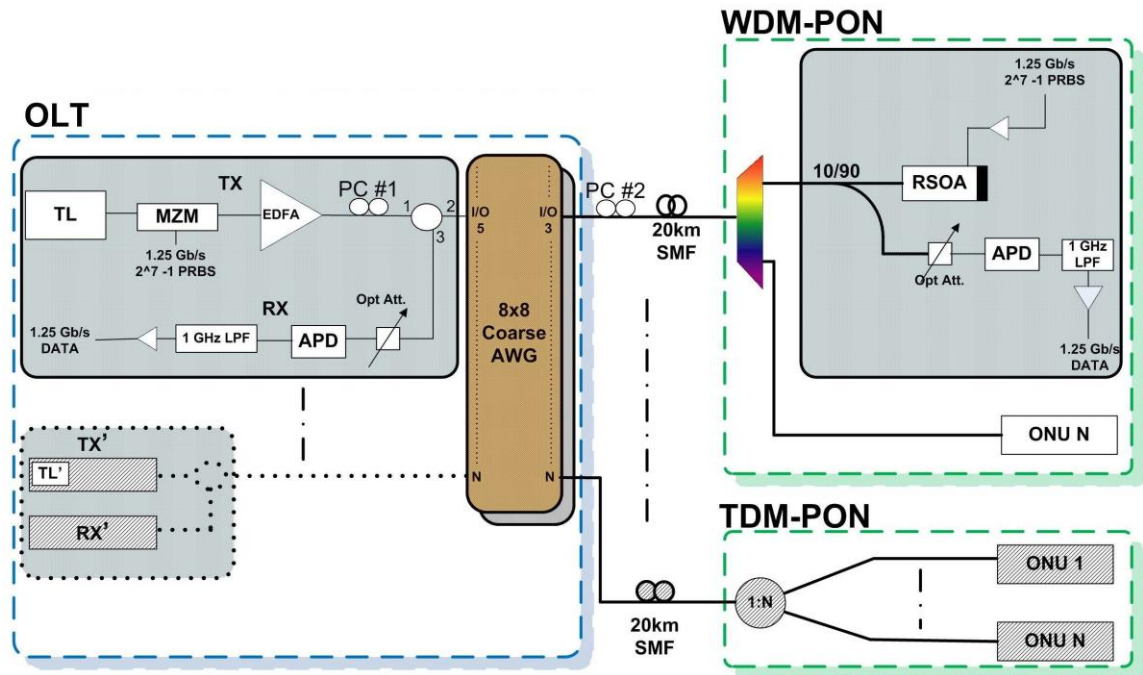


Figure 7-1 Coarse-routed PONs network architecture and experimental setup

network [1]. VPI modelling results have confirmed error-free grooming of 16, 0.4 nm-spaced ONUs of a WDM-PON over a typical, 7 nm-wide Gaussian passband window of a  $5 \times 5$  prototype AWG [2] in the presence of 0.8 nm PDW shifting and  $270^\circ$  worst case phase errors [1].

In the absence of a commercial 7 nm coarse AWG [2], currently available only in the form of prototypes, a readily-available 2.7 nm Gaussian device was employed to confirm experimentally the routing behaviour and overall performance of the central and border passband wavelengths, employed by ONUs in a WDM-PON, having displayed through simulations the least and mostly degraded error rates respectively due to the AWG polarisation dependency and effective network power distribution.

### 7.1.1 Characteristics of the readily-available 2.7 nm coarse AWG

The 8×8 AWG device used in the experimental setup, provided by Nortel, comprises 4 nm-spaced coarse channels ranging from 1520 nm to 1590 nm using 32.5 nm-wide FSRs. The measured transmission spectra of two adjacent channels around 1550 nm is displayed in Figure 7-2, exhibiting adjacent channels crosstalk isolation of 20 dB at the centre of the passband and insertion loss of approximately 5.2 dB, representing equivalent crosstalk and loss figures to the prototype modelled AWG [2].

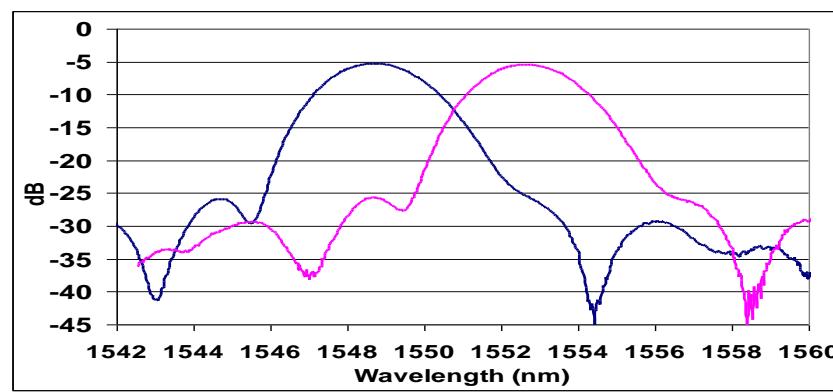


Figure 7-2 2.7 nm commercially-available coarse AWG transmission spectra

To demonstrate experimentally the coarse-fine grooming capability of the AWG, the coarse channel at  $\lambda_{\text{central}}=1552.67$  nm with a measured 2.7 nm Gaussian passband at 3 dB, and 3 wavelengths mapped within, corresponding to the central wavelength at 1552.67 nm and edge wavelengths at 1551.48 nm and 1554 nm, were employed as shown in Figure 7-3.

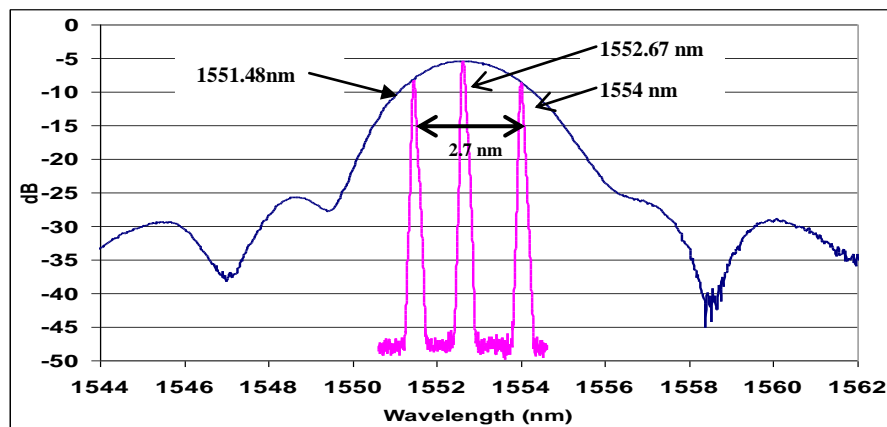


Figure 7-3 2.7 nm commercially-available AWG coarse-fine grooming spectra

### 7.1.2 Experimental setup

Specified in the experimental setup, shown in Figure 7-1, a MZM (JDSU MOD-9201) was used in the OLT to externally modulate a tunable laser (TL) source (JDS SWS15101) at 3 dBm with a 1.25 Gbit/s,  $2^7-1$  PRBS applied at the modulator's RF input to comply with the limited RSOA electrical frequency response at 1.2 GHz [3]. An EDFA was set to provide the link between the MZM and AWG at this instance, engineered to compensate for the modulator's excessive loss of 11 dB and subsequent 1.9 dB in the polarisation controller (PC#1) and circulator, providing approximately 0 dBm at the AWG input necessary to avoid driving the RSOAs in the destination ONUs in saturation at received power levels above -14 dBm. Nevertheless, the use of the EDFA is expected to be diminished when a MZM with a typical 5 dB loss is employed. Additive power losses were incurred at various points in the network as expected, including 5.2 dB at the coarse AWG, 4 dB at the SSMF and 5.5 dB at the distribution demultiplexer.

To establish bidirectional transmission for the least and most degraded ONUs [1] of a WDM-PON, two wavelengths at 1552.67 nm and 1554 nm were selected, corresponding to the centre and longest wavelengths of the AWG central channel  $\lambda_{\text{central}} = 1552.67$  nm. Following modulation, both wavelengths were applied sequentially to PC#1 to allow routing via either the TE or TM passband of the AWG and through a circulator, allowing for bidirectional transmission in the OLT, applied to AWG downstream I/O port 5, to be routed collectively as a single coarse channel to output port 3.

The AWG I/O port 3 downstream was subsequently coupled to a 20 km SSMF through PC#2, utilised to manage the RSOA's 1 dB PDG, before reaching the network distribution point, consisting of a 40-port, 0.37 nm demultiplexer (LightWeaver LMC-AWGD-W-401-01-P0R-0001), to communicate the received wavelengths to the designated ONUs. In each ONU, a

90/10 optical coupler was used to supply 90% of power to the RSOA for upstream transmission and 10% to an APD for downstream detection. To simulate upstream transmission, each injected CW at the RSOA input at -14 dBm maximum power, was initially amplified by 12.5 dB and subsequently reflected, providing upstream carriers at -1.5 dBm, to be modulated in turn by another 1.25 Gbit/s,  $2^7-1$  PRBS with measured ER of up to 9 dB, as shown in Figure 7-4, matching the simulation characteristic described in preceding chapters. Due to its grooming property, the same AWG path used in downstream will be employed by the network to transmit sequentially the reflected modulated carriers upstream. In their route, after multiplexed and transmitted over the SSMF, they would pass via PC#2 in the OLT, to engage the TE or TM passbands of the AWG and due to the AWG Latin property, terminated through the circulator to a common APD.



Figure 7-4 Extinction ratio of the experimental RSOA transmitted signal

## 7.2 Routing performance experimental results

To experimentally demonstrate collective upstream routing at PON level, aiming to verify the routing simulation results produced in section 4.3, three wavelengths were initiated sequentially in two successive coarse channels  $\lambda_{\text{central}}=1552.67$  nm and  $\lambda_{\text{central-1}}=1548.8$  nm using a single tunable laser, to represent ONUs of two distinctive WDM-PONs connected at upstream ports 3 and 4 of the AWG respectively. Figure 7-5 shows the displayed spectra at the respective AWG input ports and corresponding output port 5, following the Latin routing. Experimental results indicate that all 3 wavelengths representing each PON are routed through the relevant AWG coarse channels to a common destination with a maximum 3 dB power variation among them due to the passbands Gaussian response. In that sense, confirming in practice the ability of the architecture to accommodate various physical PON locations in a single port of its passive router concurrently with the use of a single transceiver between the OLT and ONUs [4], allowing for network scalability to handle PON upgrade, increased network penetrations and transparency in the sense of PON technologies.

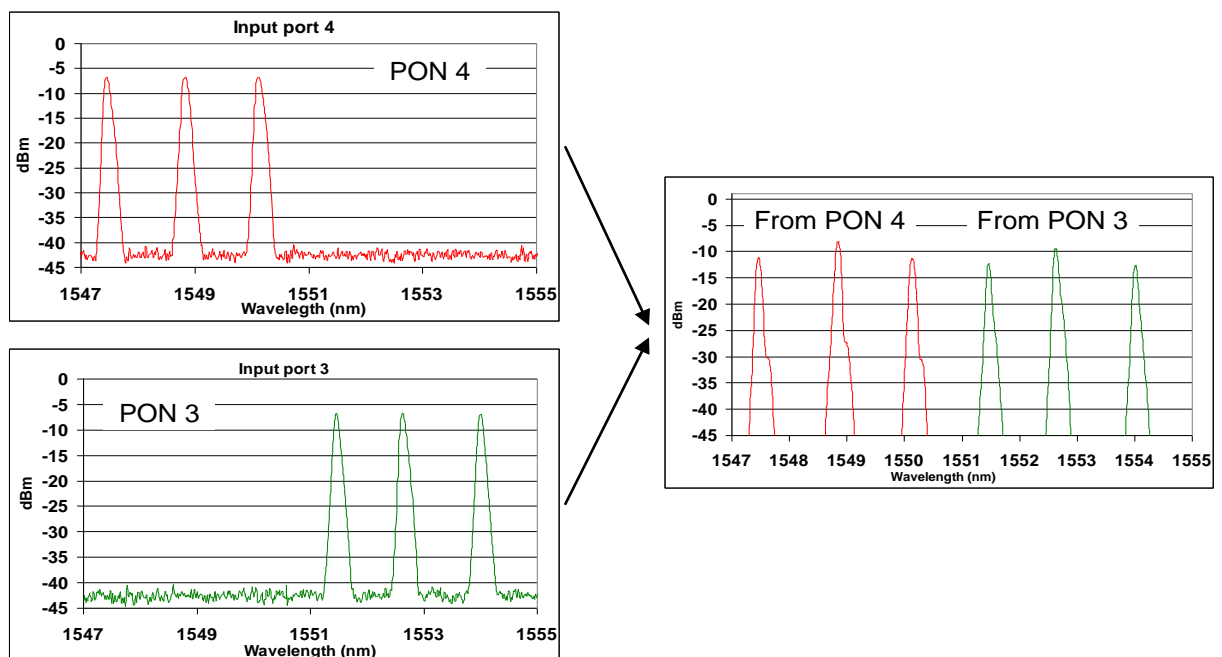
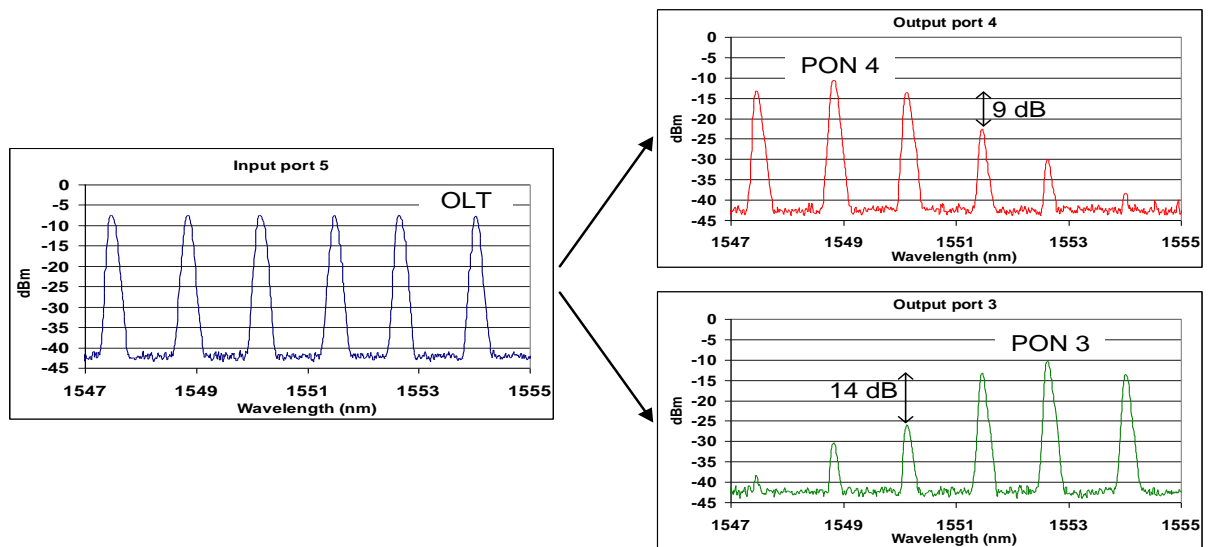


Figure 7-5 Commercially-available AWG input and output ports upstream spectra

Alternatively, to assess downstream performance, Figure 7-6 shows the measured spectrum plots of the AWG input port 5 and corresponding output ports 3 and 4. Results validate their simulation counterparts, where downstream wavelengths at the OLT are successfully routed through distinctive coarse channels to their designated outputs according simply to OLT and individual PON physical terminations purely due to the designed coarse-fine grooming.



**Figure 7-6** Commercially-available AWG input and output ports downstream spectra

Despite the inherited AWG adjacent channel crosstalk isolation of 20 dB, shown in Figure 7-2, it exhibits reduced crosstalk isolation of 9 dB at the passband edge of PON 4 as a result of crosstalk with wavelengths designated for the adjacent PON 3, as shown in Figure 7-6. This relatively low figure is further compensated by an extra isolation of the successive network distribution element in a WDM-PON.

### 7.3 Evaluation of passband shifting in downstream and upstream

To demonstrate the polarisation dependency of the AWG passbands to transmitted wavelengths and, to that effect determine the overall coarse channel shifting and associated wavelength PDL, the experimental AWG was initially scanned with the help of an EDFA, polarisation beam splitter and controller in both directions of transmission to identify possible imbalances in individual passband responses. Figure 7-7 displays the downstream and upstream passbands of coarse channel  $\lambda_{\text{central}} = 1552.67$  nm, for which the TM response is shifted by -0.15 nm and -0.35 nm respectively with respect to TE. Although these values, as expected, lack considerably the symmetrical 0.8 nm shifting of prototype coarse AWGs [2, 5], simply due to the restricted 2.7 nm passband as opposed to 7 nm typical, they represent comparable shifting as a percentage of the overall AWG passband width and as a result constitute an efficient measure of network performance due to PDL.

Figure 7-7(a) in particular shows a moderate PDL difference between the central and longest downstream transmitted wavelengths at 1552.67 nm and 1554 nm extended from 0.2 dB to approximately 0.8 dB respectively. In addition to the measured PDL figures, the AWG Gaussian response has contributed to the overall attenuation resulting to maximum 5.4 dB and 9 dB losses reported for the centre and longest wavelengths respectively. In upstream and due

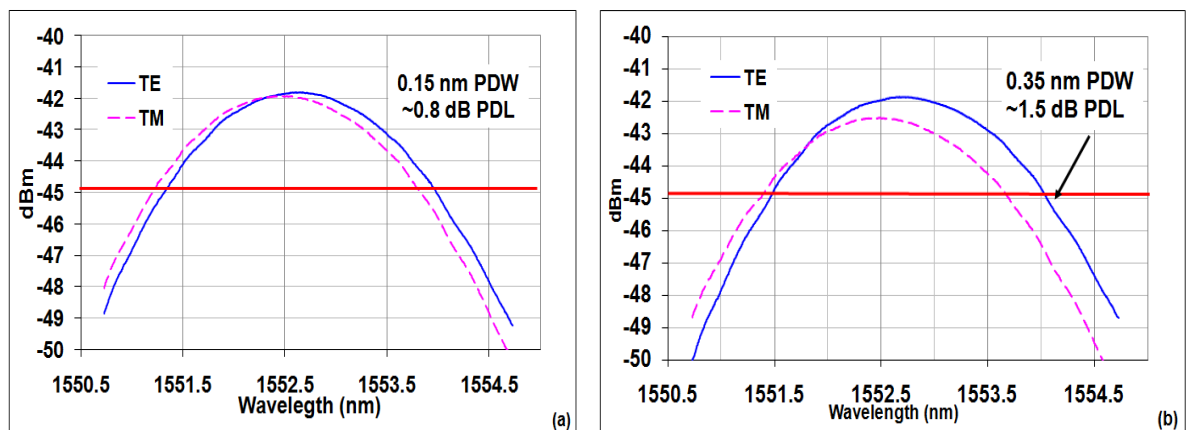


Figure 7-7 passband shifting of the experimental AWG channel in (a) downstream and (b) upstream

to the increased PDW shift displayed in Figure 7-7(b) as a result of the device imbalance, total PDLs of approximately 0.8 dB and 1.5 dB were recorded for the centre and longest wavelengths imposing slight higher overall attenuation figures of 6 dB and 9.7 dB respectively.

## 7.4 Bidirectional transmission and Rayleigh backscattering interference

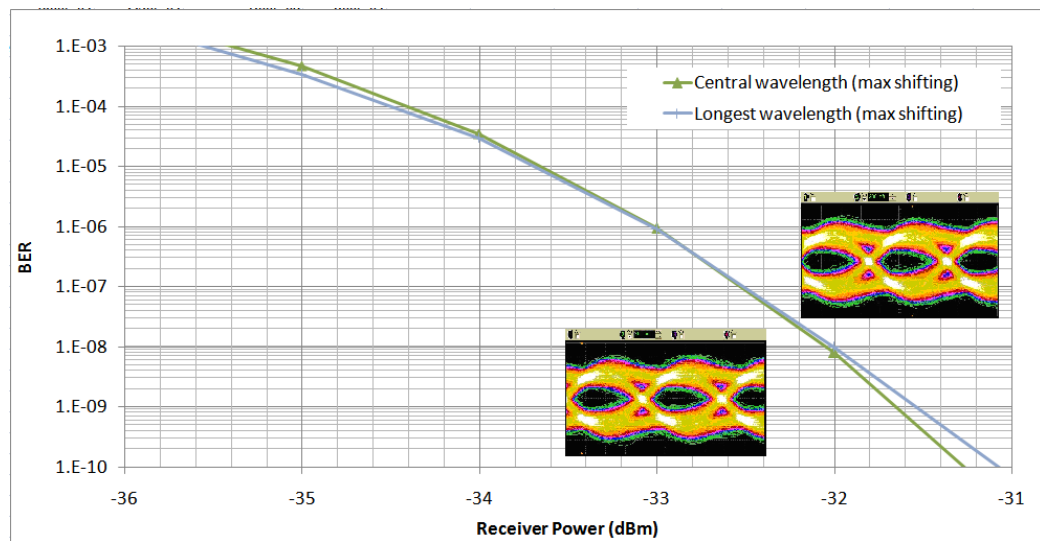
The network is designed in terms of power budgeting to compensate in particular for the excessive losses of the MZM, as opposed to the simulation model considering typical loss figures, and the gain of the RSOAs, expected to be critical in displaying error-free transmission of all wavelengths of a WDM-PON. Analysis of power budget measurements for the most and least severely degraded ONU at maximum PDW shift is summarised in Table 7-1.

Table 7-1 Network power budget

Parameter	Value	
TL launched power	3 dBm	
MZM insertion loss	11 dB	
EDFA output power	2.5 dBm	
Optical circulator & PC#1 connector losses	1.9 dB	
Coarse AWG loss	9 dB @ longest wavelength 5.4 dB @ central wavelength	
20 km SSMF loss	4 dB	
Distribution point multiplexer loss	5.5 dB	
Optical 90/10 coupler	1 dB	13 dB
RSOA gain	12.5 dB	
APD sensitivity @ $10^{-9}$ error-rate		-31.5 dBm
RSOA reflected power @ longest wavelength	-5.3 dBm	
Upstream network losses	20.2 dB	
APD sensitivity @ $10^{-9}$ error-rate	-27.5 dBm	

According to Table 7-1 the highest link loss specified in downstream between the EDFA output in the OLT and the APD in the ONU, measured 21.7 dB, was recorded as expected for the longest wavelength with an optical circulator, multiple connectors, the coarse AWG, 20 km SSMF, a distribution point multiplexer and a 90/10 optical coupler on route. Yet, the power budget has allowed for at least 1.5 dB safety margin. In upstream, the highest link loss recorded between the RSOA in the ONU and the APD in the OLT again for the longest wavelength, measured 20.2 dB, with at least 2.5 dB safety margin.

To evaluate network performance, downstream BER responses are drawn in Figure 7-8 for the centre and longest wavelengths, representing different ONUs of the experimental WDM-PON. Downstream plots confirm error-free transmission for all ONUs with measured BERs of  $10^{-9}$  at a trivial 0.2 dB power penalty between the centre and longest wavelengths due to a 0.15 nm PDW shift.



**Figure 7-8** Measured BER for downstream transmission at central and longest wavelength

An equally acceptable BER performance was also achieved in upstream as shown in Figure 7-9 at an increased power penalty of up to 3 dB between the central wavelength with no PDW shift and the longest wavelength at the worst case 0.35 nm PDW shift. This penalty is expected to be reduced in a practical system by power equalisation in the OLT [6] since it was caused by a variation of 3.8 dB in the RSOA injected power at the longest wavelength leading to lower ER. It can also be observed that there is an insignificant 0.2 dB penalty between the central and longest wavelengths with no PDW shift, despite the inevitable 3 dB difference in power in both downstream and upstream paths due to the AWG Gaussian response. This is mostly important since the prospect of using a polarisation-independent coarse AWG will have great potential to allow bidirectional transmission with negligible penalty. In addition, the polarisation independency of the RSOA [3] can be verified from the 0.2 dB penalty between the back-to-back transmissions via the TE and TM gain curves of the device.

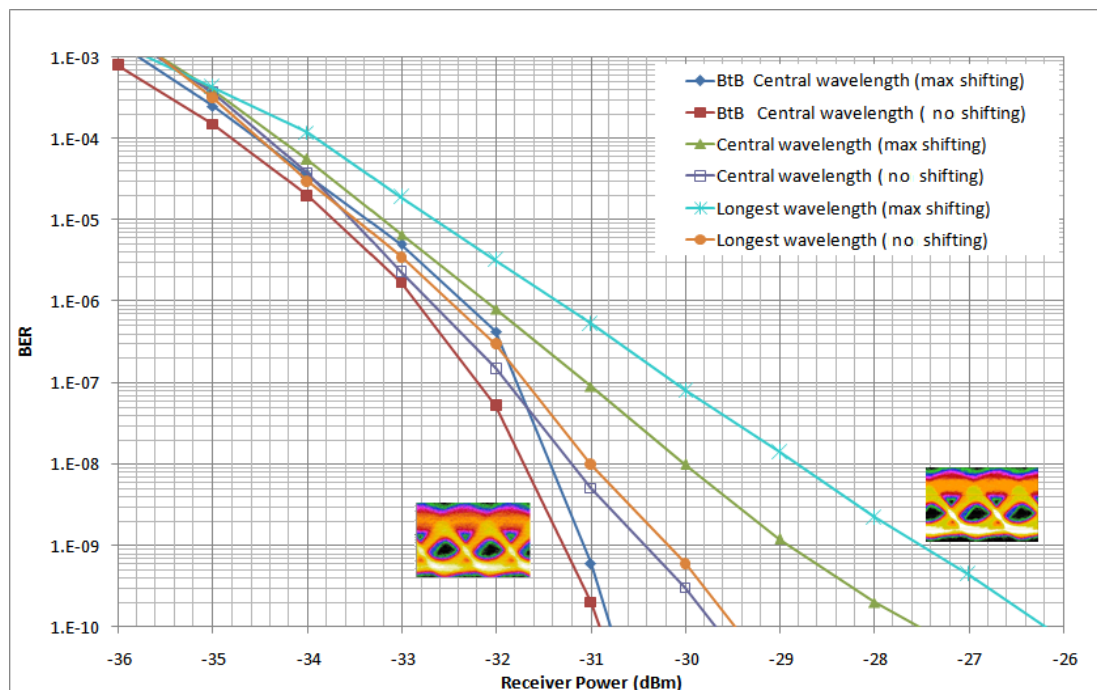


**Figure 7-9 Measured BER for upstream transmission at central and longest wavelength**

Finally, since bidirectional transmission for each ONU is achieved by using the same wavelength, Rayleigh backscattering (RBS) and back reflections from the AWG connectors may become crucially important [7]. To verify the impact of these reflections, the AWG back reflections at the input of the APD in the OLT for the centre and longest wavelengths were measured and shown in Figure 7-10 (a) and (b) respectively. It can be observed that the back reflections are coherent with optical power levels of -45 dBm and -54 dBm for the central and longest wavelengths respectively, exhibiting 9 dB difference in power between the two wavelengths due to the Gaussian response and PDL, induced twice both in downstream and upstream. To reduce the AWG reflections by approximately 15 dB, the AWG ports used in the experiment were fused with angular phase connectors (APCs) to moderate reflectance of the connections [7], while all the unused ports were index-matched using a glycerine bath to decrease reflectance collectively without the need to fuse a large number of APCs.

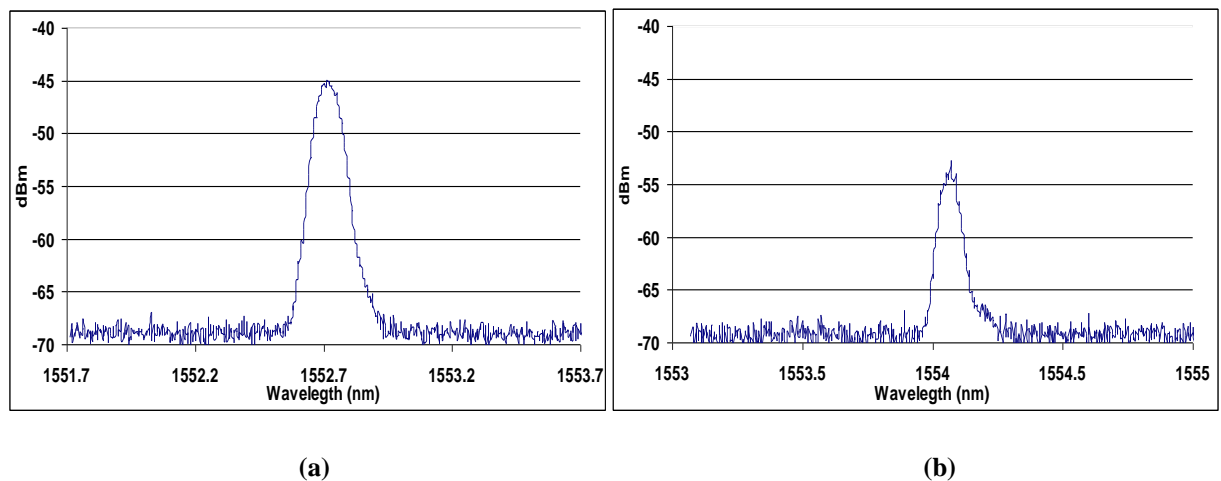


**Figure 7-10** Experimental AWG reflections at APD input in the OLT at (a) central (b) longest wavelengths

Subsequently, Figure 7-11 demonstrates the measured signal power distribution and RBS power levels in each point of the network. The total RBS in the OLT originates firstly in the unmodulated optical carrier travelling downstream and secondly in the modulated signal travelling upstream [8]. The latter passes back to the RSOA where it is reflected and amplified, subsequently propagating simultaneously with the signal in the upstream direction. As a result, total RBS power levels of -36dBm and -40 dBm for the central and longest wavelengths respectively were recorded at the 20 km fibre-end upstream, as shown in Figure 7-11. Subsequently, combined with the AWG back-reflections, the total reflection power levels towards the receiver in the OLT were measured to reach -40.65 dBm and -44.9 dBm, allowing also for upstream signal to total reflection power ratios of 23.65 dB and 20.4 dB for the central and longest wavelengths respectively. These figures clearly suggest that RBS and back reflections from the AWG do not impose a limitation to the network performance since they provide sufficient power ratio to allow error-free detection in the OLT. The major contributors to such moderate RBS and back reflection figures are considered to be the distribution of network elements [9] in the proposed architecture and the inherited power budgeting controlled by the combination of RSOA amplification and maximum PDW shift upstream.

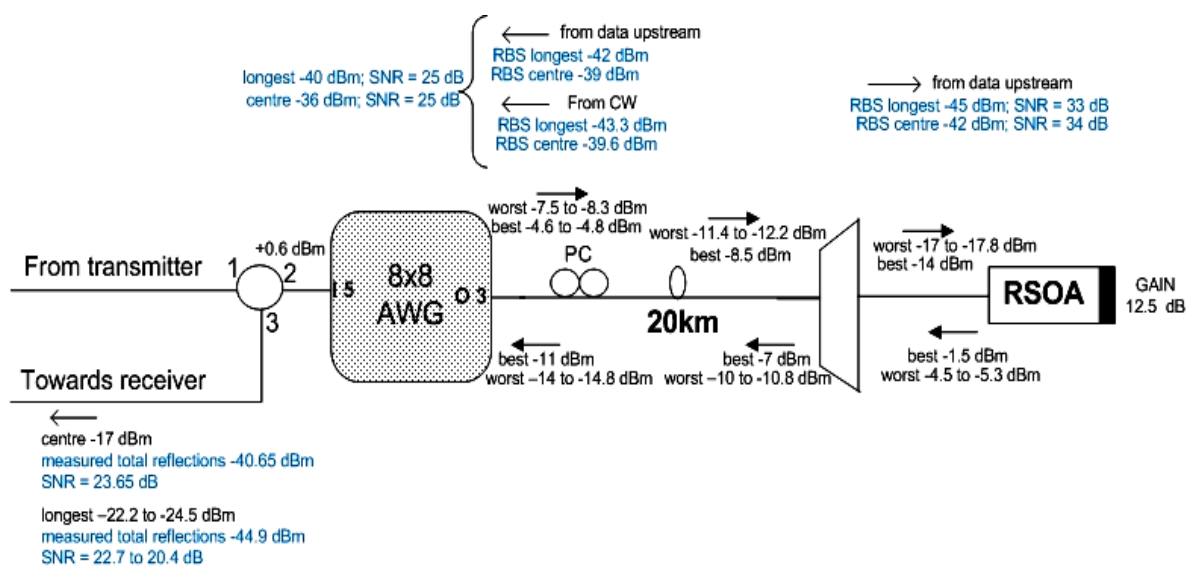


Figure 7-11 Network bidirectional and Rayleigh backscattering power distribution

## 7.5 Summary

This chapter summarised the performance figures produced by the experimental demonstration of coarse-fine grooming over a practical implementation of the access network proposed in proceeding chapters. This was achieved mainly by the application of a readily-available 2.7 nm-wide Gaussian channel AWG with the aim to substantiate the simulation results that recommended the feasibility and performance validity of the original network architecture analysed in this thesis.

Initially, the AWG grooming characteristic and its potential to route jointly multiple ONUs of distinctive WDM-PONs with maximum power variations among them of up to 3 dB was demonstrated at  $\lambda_{\text{central}}=1552.67$  nm. Significantly, multiple AWG channel operation displayed no more than 9 dB crosstalk figures between adjacent PON channels that have been considerably compensated for the potentially affected boarder wavelengths among coarse channels by the distribution point multiplexer adjacent wavelength crosstalk isolation figure of 25 dB.

Experimental results have confirmed  $10^{-9}$  routing for the most severely degraded ONUs transmitted at the edge of the experimental AWG 2.7 nm-wide Gaussian passband, accounting for 0.35 nm PDW shift and 1.5 dB maximum PDL. Further analysis, based on power budgeting and more than 20 dB measured signal to reflections noise suggests that Rayleigh crosstalk is not limiting the bidirectional transmission, demonstrating the feasibility of accommodating fully-populated WDM and TDM-PONs when current 7 nm-wide coarse AWGs prototypes become commercially-available. Significantly, the use of a single OLT to access various physical PONs in 20 km proximity with multiple wavelengths allows for network scalability by means of increased network penetration, ONU update and interoperability of PON technologies.

## 7.6 References

- [1] Y. Shachaf, P. Kourtessis, and J. M. Senior, "An interoperable access network based on CWDM-routed PONs," presented at 33rd European Conference and Exhibition on Optical Communication (ECOC), Berlin, Germany, 2007.
- [2] J. Jiang, C. L. Callender, C. Blanchetière, J. P. Noad, S. Chen, J. Ballato, and J. Dennis W. Smith, "Arrayed Waveguide Gratings Based on Perfluorocyclobutane Polymers for CWDM Applications," *IEEE Photonics Technology Letters*, vol. 18, pp. 370-372, 2006.
- [3] CIP-Photonics,  
["http://www.ciphotonics.com/PDFs%20May08/SOA\\_RL\\_OEC\\_1550\\_J.pdf,"](http://www.ciphotonics.com/PDFs%20May08/SOA_RL_OEC_1550_J.pdf) 2008.
- [4] Y. Shachaf, P. Kourtessis, and J. M. Senior, "Multiple - PON access network architecture," presented at IEEE/IET 2nd International Access Technologies (ICAT), Cambridge, UK, 2006.
- [5] H. C. Woei, N. A. Rahman, and S. Shaari, "Conventional Arrayed Waveguide Grating with 4 Channel Structure Design for CWDM," presented at International Conference on Semiconductor Electronics (ICSE), Kuala Lumpur, Malaysia, 2004.
- [6] P. Youngil, L. Chunghwan, and J. Inkwun, "ONU power equalization of ethernet PON systems," *IEEE Photonics Technology Letters*, vol. 16, pp. 1984-1986, 2004.
- [7] J. Prat, C. Arellano, V. Polo, and C. Bock, "Optical Network Unit Based on a Bidirectional Reflective Semiconductor Optical amplifier for Fiber-to-the-Home Networks," *IEEE Photonics Technology Letters*, vol. 17, pp. 250-253, 2005.
- [8] E. K. MacHale, G. Talli, and P. D. Townsend, "10Gb/s bidirectional transmission in a 116km reach hybrid DWDM-TDM PON," presented at Optical Fiber Communication and the National Fiber Optic Engineers Conference (OFC/NFOEC 2006), Anaheim, USA, 2006.

- [9] C. Arellano, V. Polo, and J. Prat, "Effect of the Multiplexer Position in Rayleigh-Limited WDM-PONs with Amplified-Reflective ONU," presented at 9th International Conference on Transparent Optical Networks (ICTON '07), 2007.